



This is a repository copy of *Reduced palmitoylation of SQSTM1/p62 in Huntington disease Is associated with impaired autophagy.*

White Rose Research Online URL for this paper:

<https://eprints.whiterose.ac.uk/226528/>

Version: Published Version

Article:

Abrar, F., Davies, M.C., Alshehabi, Y. et al. (10 more authors) (2025) Reduced palmitoylation of SQSTM1/p62 in Huntington disease Is associated with impaired autophagy. *The FASEB Journal*, 39 (9). e70549. ISSN 0892-6638

<https://doi.org/10.1096/fj.202401781r>

Reuse

This article is distributed under the terms of the Creative Commons Attribution-NonCommercial-NoDerivs (CC BY-NC-ND) licence. This licence only allows you to download this work and share it with others as long as you credit the authors, but you can't change the article in any way or use it commercially. More information and the full terms of the licence here: <https://creativecommons.org/licenses/>

Takedown

If you consider content in White Rose Research Online to be in breach of UK law, please notify us by emailing eprints@whiterose.ac.uk including the URL of the record and the reason for the withdrawal request.



eprints@whiterose.ac.uk
<https://eprints.whiterose.ac.uk/>

RESEARCH ARTICLE **OPEN ACCESS**

Reduced Palmitoylation of SQSTM1/p62 in Huntington Disease Is Associated With Impaired Autophagy

F. Abrar¹ | M. C. Davies² | Y. Alshehabi¹ | A. Kumar¹ | A. Dang¹ | Y. T. N. Nguyen³ | J. Collins³ | N. S. Caron³ | J. S. Choudhary⁴ | S. S. Sanders³ | M. O. Collins²  | M. R. Hayden³ | D. D. O. Martin¹ 

¹Department of Biology, University of Waterloo, Waterloo, Ontario, Canada | ²Molecular and Cell Biology Cluster, School of Biosciences, University of Sheffield, Sheffield, UK | ³Department of Medical Genetics, BC Children's Hospital Research Institute, Centre for Molecular Medicine and Therapeutics, University of British Columbia, Vancouver, British Columbia, Canada | ⁴Cancer Biology Division, Functional Proteomics, Chester Beatty Laboratories, The Institute of Cancer Research, London, UK

Correspondence: M. O. Collins (mark.collins@sheffield.ac.uk) | D. D. O. Martin (dale.martin@uwaterloo.ca)

Received: 1 August 2024 | **Revised:** 10 March 2025 | **Accepted:** 9 April 2025

Funding: This work was supported by The Royal Society (RG150409) and Natural Sciences and Engineering Research Council of Canada (NSERC) (RGPIN-2019-04617).

ABSTRACT

Disruption of autophagy has emerged as a common feature in many neurodegenerative diseases. Autophagy is a membrane-dependent pathway that requires many key regulators to quickly localize on and off membranes during induction, promoting membrane fusion. Previously, our bioinformatic approaches have shown that autophagy and Huntington disease (HD) are enriched in palmitoylated proteins. Palmitoylation involves the reversible addition of long-chain fatty acids to promote membrane binding. Herein, we show that inhibition of palmitoylation regulates the abundance of several key regulators of autophagy and leads to a partial block of autophagic flux. We confirm that the autophagy receptor SQSTM1/p62 (sequestosome 1) is palmitoylated and directed to the lysosome. Importantly, we report that SQSTM1 palmitoylation is significantly reduced in HD patient and mouse model brains. This finding reveals a novel mechanism contributing to the generation of empty autophagosomes previously seen in HD models and patient-derived cells.

1 | Introduction

Protein mislocalization and proteostasis deficiency are hallmarks of neurodegeneration [1–3]. The cell has two primary ways to eliminate misfolded and aggregated proteins: the unfolded protein response and autophagy. The unfolded protein response requires the proteasome but quickly becomes overwhelmed in diseases such as Huntington disease (HD), amyotrophic lateral sclerosis (ALS), and other neurodegenerative diseases [2, 4–6]. As such, autophagy then becomes the bulk protein clearance pathway. Autophagy generally refers to a pathway that allows the delivery of damaged or superfluous organelles and aggregated proteins to the lysosome

for degradation and recycling [7]. Autophagy can be further classified into three broad categories: macroautophagy (hereafter referred to as autophagy), chaperone-mediated autophagy (CMA), and microautophagy [7]. A common theme among these pathways is that they involve dynamic changes in membranes and/or protein interactions with those membranes. However, in many cases, how autophagy regulators quickly transition from the cytosol to membranes is generally unknown or overlooked.

Previously, we conducted the first unbiased bioinformatics analysis showing that S-acylation of proteins is enriched in neurodegenerative diseases and proteostasis deficiencies,

F. Abrar and M.C. Davies contributed equally to this article.

This is an open access article under the terms of the [Creative Commons Attribution-NonCommercial-NoDerivs](https://creativecommons.org/licenses/by-nc-nd/4.0/) License, which permits use and distribution in any medium, provided the original work is properly cited, the use is non-commercial and no modifications or adaptations are made.

© 2025 The Author(s). *The FASEB Journal* published by Wiley Periodicals LLC on behalf of Federation of American Societies for Experimental Biology.

including HD and ALS [8]. S-acylation refers to the reversible and covalent addition of saturated fatty acids to cysteine residues through a thioester bond [8, 9]. The most common form involves palmitate and is generally referred to as S-palmitoylation, or simply palmitoylation. The hydrophobic moiety is primarily involved in membrane binding but can also promote protein–protein interactions, conformational changes, or protein folding [10, 11]. Much like phosphorylation, palmitoylation is reversible and dynamic and is regulated by a diverse set of enzymes that add or remove palmitate from proteins. The fatty acid moiety is added by palmitoyl acyltransferases (PATs) and removed by the serine hydrolases of the acyl protein thioesters (APTs), protein palmitoyl thioesterases (PPT), and the α/β -hydrolase domain (ABHD) protein families [12–16]. Thus, palmitoylation provides an ideal mechanism for quickly redirecting proteins on and off membranes. When S-acylation is disrupted, it leads to protein mislocalization, decreased protein turnover, and aggregation [5].

Previous work has implicated a potential role for palmitoylation in autophagy [17, 18]. Palmitate treatment increases LC3-I to LC3-II conversion and decreases SQSTM1 levels, all signs that autophagy levels are increased [8]. The use of the tandem LC3 reporter with palmitate treatment shows a decrease in the number of autophagosomes and an increase in autolysosomes [18]; again, indicating an overall increase in autophagy and highlighting a link between palmitoylation and autophagy. In addition, we recently showed that the majority of autophagy regulatory genes encode a proteoform that has been detected by low- or high-throughput methods [5], by comparing the S-acylation database SwissPalm [19] and the Autophagy Regulatory Network [20].

Autophagy induction requires the recruitment of MCOLN3/TRPML3, a Ca^{2+} -permeable cation channel, to provide Ca^{2+} for autophagosome biogenesis [17]. It was recently shown that this channel requires palmitoylation at the C-terminus, a modification essential for the trafficking and function of the channel in autophagy. When HeLa cells are starved of nutrients, MCOLN3/TRPML3 is activated alongside palmitoylation, with palmitoylation disruption resulting in the activation of MCOLN3/TRPML3 and autophagy being abolished [17]. Recently, we identified multiple components of the MTOR complex 1 that are palmitoylated in human embryonic kidney 293T (HEK293T) cells [21]. Again, this work implicates a direct role of palmitoylation in autophagy. However, further investigation of the exact role palmitoylation plays in the regulation of autophagy is needed.

Herein, we show that S-acylation may provide a mechanism for autophagy regulators to rapidly and reversibly bind on and off membranes. Furthermore, we find that the autophagy receptor SQSTM1/p62 is S-acylated and directed to the lysosome. These findings were recently confirmed by Yang and colleagues [22]. In this study, we show that SQSTM1 S-acylation is significantly reduced in HD patient and mouse model brains. This finding may provide a mechanism for the production of empty autophagosomes previously seen in HD models and patient cells [23, 24].

2 | Materials and Methods

2.1 | Materials

This study examined de-identified archived brain tissue samples from the Huntington Disease BioBank at the University of British Columbia. All samples were collected, stored, and accessed with informed consent and approval of The University of British Columbia/Children's and Women's Health Centre of British Columbia Research Ethics Board (UBC C&W REB H06-70467 and H06-70410). Tissues used were from patients of similar age at death, CAG size, and post-mortem intervals. Male and female samples were included in controls and diseased samples. HA-tagged SQSTM1 and RFP-LC3 were gifts from Qing Zhong (Addgene, 28027) [25] and Tamotsu Yoshimori (Addgene, 21075) [26], respectively. All point mutations for SQSTM1-HA were generated by site-directed mutagenesis by TopGene Biotech (Ontario, Canada). Cathepsin B-BFP (CTSB-BFP) was a kind gift from the Davidson laboratory stocks. Unless otherwise indicated, all antibodies were acquired from Cell Signaling Technology or Millipore-Sigma.

2.2 | Mice

All mouse experiments were carried out in accordance with protocols approved by the UBC Committee on Animal Care and the Canadian Council on Animal Care (Animal protocol A07-0106). Mice were derived from in-house breeding pairs, maintained under a 12h light:12h dark cycle in a clean facility, and given free access to food and water, except where indicated (for fasting). As previously described, mice were fasted for 24h with full access to water to induce autophagy in the brains [27]. YAC128 mice were on an FVB/N background, and mixed sexes were analyzed (no sex differences were observed).

2.3 | Statistics

Unless otherwise indicated, statistical significance was assessed using Student's *t*-test for comparison of two groups, one-way ANOVA with post hoc Tukey's correction for the comparison of one variable between more than two groups, and two-way ANOVA with post hoc Bonferroni correction for the comparison of two variables between groups. Variances between groups were similar. All analyses were performed using the GraphPad Prism 5.01 or higher software package. Graphs are presented as the standard error of the mean (SEM).

2.4 | Cell Culture and SILAC Labelling

HeLa cells were grown in normal DMEM (Gibco) supplemented with 1% penicillin–streptomycin (Gibco). Where indicated, induction of autophagy in HeLa cells was conducted by the application of Earle's Balanced Salt Solution (EBSS; Thermo Fisher, 24010043). Inhibition of autophagy was conducted by the application of 500nM bafilomycin A₁ (BafA1; Alfa Aesar, J61835).

For SILAC experiments, DMEM lacking lysine and arginine (Dundee Cell Products) was supplemented with 40 mg/L lysine and 84 mg/L arginine of normal, light isotopic composition (Sigma) for the K0/R0 population, and heavy isotopes (4, 4, 5, 5-D4 L-lysine and 13C6 L-arginine, Cambridge Isotope Laboratories (CIL)) for the K4/R6 population. The medium was supplemented with 10% FBS (Gibco) that had been dialyzed at 1 kDa (SpectraPor) overnight in 150 mM NaCl to remove traces of normal weight isotopic amino acids. HeLa cells were treated with either DMSO (Light, K0/R0) or 50 μ M palmostatin B (heavy K4/R6) for 18 h.

2.5 | Quantitative Proteome Profiling of Drug-Treated Cells

Cell pellets from each condition were lysed with a 4% SDS-containing extraction buffer, as previously described [28], and pooled, and 3 biological replicates were prepared and analyzed for each treatment group. Thirty μ g of each pooled sample was separated on a 12% SDS-PAGE gel to fractionate proteins for quantitative proteome profiling. Protein gels were stained overnight with colloidal Coomassie Brilliant Blue (Sigma). Each lane was excised into 9 sections, which were destained and in-gel digested overnight using trypsin (sequencing grade; Roche). Peptides were extracted from gel bands twice with 50% acetonitrile: 0.5% formic acid and dried in a SpeedVac (Thermo). Peptides were resuspended in 0.5% formic acid and were analyzed by LC-MS/MS analyses using an Ultimate 3000 RSLC Nano LC System (Dionex) coupled to an LTQ Orbitrap Velos hybrid mass spectrometer (Thermo Scientific) equipped with an Easy-Spray (Thermo Scientific) ion source. Peptides were desalted on-line using a capillary trap column (Acclaim Pepmap100, 100 μ m, 75 μ m \times 2 cm, C18, 5 μ m (Thermo Scientific)) and then separated using a 180 min RP gradient (4%–30% acetonitrile/0.1% formic acid) on an Acclaim PepMap100 RSLC C18 analytical column (2 μ m, 75 μ m id \times 50 cm, [Thermo Scientific]) with a flow rate of 0.3 μ L/min. The mass spectrometer was operated in standard data-dependent acquisition mode controlled by Xcalibur 2.2. The instrument was operated with a cycle of one MS (in the Orbitrap) acquired at a resolution of 60 000 at m/z 400, with the top 15 most abundant multiply-charged (2+ and higher) ions in a given chromatographic window subjected to CID fragmentation in the linear ion trap. An FTMS target value of 1e6 and an ion trap MSn target value of 10 000 were used. Dynamic exclusion was enabled with a repeat duration of 30 s, with an exclusion list of 500 and an exclusion duration of 60 s. Lock mass of 401.922 was enabled for all experiments.

2.6 | Mass Spectrometry Data Analysis

Data were analyzed using MaxQuant version 1.4.1.2. The MaxQuant processed data were searched against a UniProt (downloaded October 2014) human sequence database using the following search parameters: trypsin with a maximum of 2 missed cleavages, 7 ppm for MS mass tolerance, and 0.5 Da for MS/MS mass tolerance, with acetyl (Protein N-term) and oxidation (M) as variable modifications and carbamidomethyl (C) as a fixed modification. Light (K0/R0) and heavy (K4/R6) SILAC

labels were specified for SILAC quantification. A protein FDR of 0.01 and a peptide FDR of 0.01 were used for identification level cutoffs. Match between runs with a 2-min retention time window was enabled. Data were filtered so that at least 3 valid normalized SILAC ratios were present, and two sample *t*-testing was performed with a permutation-based FDR calculation in Perseus (1.4.1.3).

2.7 | Palmitoylation Assays

Palmitoylation using the acyl-resin assisted capture (Acyl-RAC) and immunoprecipitation acyl-biotin exchange (IP-ABE) assays was detected, as described previously [29–31]. Briefly, cells were lysed in the presence of 100 mM NEM and incubated at 4°C overnight to alkylate free thiols. Following chloroform-methanol precipitation, 150 μ g of lysate was used to react with the thiol reactive acyl-resin assisted capture beads (Thiopropyl Sepharose 6B, T8387) in the presence of hydroxylamine (HAM), which facilitates the exchange of thioester-linked fatty acids with beads. Detection of SQSTM1 palmitoylation was achieved using the mouse anti-SQSTM1/p62 (MBL, M162-3) antibody. For IP-ABE of endogenous SQSTM1, the protein was immunoprecipitated using the same antibody and detected with rabbit anti-SQSTM1 (Enzo Life Sciences, BML-PW9860). For HA-tagged proteins, SQSTM1-HA was immunoprecipitated with rat anti-HA (3F10) and detected with mouse anti-HA (12CA5). Palmitoylation was detected using Alexa Fluor 680-conjugated streptavidin (Invitrogen, S-32358).

2.8 | Microscopy

2.8.1 | Endogenous SQSTM1 and Tandem LC3 Reporter

Cells were cultured in 12-well plates (Greiner Bio-One—665180) containing coverslips (VWR—631-0152) until ~70% confluence. Media was removed, and cells were washed with PBS three times before cells were fixed with 4% PFA (Sigma-Aldrich—158127) or ice-cold 100% methanol (VWR—BDH1135-4LG) for 20 min at room temperature (RT). Washing in PBS was conducted before permeabilization with PBS +0.3% Triton X-100 for 15 min or ice-cold 100% methanol. Cells were washed before blocking in PBS +0.01% Triton X-100 and 0.2% fish skin gelatin (Sigma-Aldrich—G7765) for 1 h at RT. Blocking buffer was removed, and the primary antibody was applied in the blocking solution for 1 h at RT or 4°C overnight. Cells were washed in PBS three times, then the fluorescent secondary antibody was applied in blocking solution for 2 h in the dark. Cells were washed in PBS three times before a final wash in dH₂O. Coverslips were removed from wells and air-dried before inversion onto DAPI-Fluoromount-G (Southern Biotech, 0100) on microscopy slides (J. Melvin Freed Brand, 7525M). Imaging was performed at the Wolfson Light Microscopy Facility at The University of Sheffield using a NIKON A1 Confocal Microscope. The following wavelengths were used: 405 nm (blue), 488 nm (green), 561 nm (red), and 595 nm (cyan). Images were acquired using a 60 \times objective lens and the NIS elements program (Nikon instruments) in an ND2 format. For all samples, no primary and no secondary controls were used to threshold the exposure

at each individual laser wavelength. Puncta were counted in FIJI using the Cell Counter (Version—ImageJwin-64) [32]. Results were analyzed on GraphPad Prism 7. Statistical significance was accepted at $p < 0.05$. Results are reported as means \pm standard error of the mean.

2.8.2 | Localization of SQSTM1-HA

HeLa cells were plated on poly-D-lysine-coated glass coverslips and transfected with SQSTM1-HA and RFP-LC3 using XtremeGene (Roche) or DNA precipitation, as previously described [33]. Where indicated, lysosomes were stained with 50 nM LysoTracker Far Red (ThermoFisher Scientific, L12492) for 1 h prior to fixation. Cells were either grown in complete media (fed) as control or subjected to growth in serum-deprived media (fasted) for 4 h to induce autophagy and visualized by confocal microscopy. Cells were fixed in 4% paraformaldehyde. Rat anti-HA and anti-rat Alexa Fluor 488 were used to detect SQSTM1-HA and imaged on an SP8 Leica microsystems confocal microscope.

3 | Results

3.1 | Inhibition of Depalmitoylation Disrupts Autophagy

To assess the extent of regulation of the autophagy network by palmitoylation, we measured changes in the proteome in response to global inhibition of depalmitoylation enzymes. Light and heavy SILAC labeled HeLa cells were treated with 0.1% DMSO as a control or the depalmitoylation inhibitor 100 μ M palmostatin B for 18 h. Quantitative mass spectrometry of tryptic digests from replicate sets of control and palmostatin B samples revealed that 273 proteins were increased in abundance after palmostatin B treatment (Table S1 and Figure 1). Out of the top 15

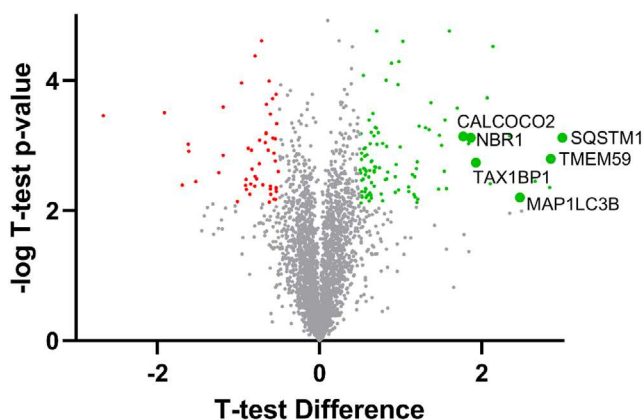


FIGURE 1 | Palmostatin B treatment upregulates components of the autophagy pathway. Volcano plot of protein abundance changes in response to treatment of HeLa cells with 100 μ M palmostatin B for 18 h. Control and palmostatin B-treated cells were SILAC labeled with light (K0/R0) and heavy (K4/R6) isotope labeled lysine and arginine to enable precise quantification of protein abundance changes. Significantly regulated proteins (red and green) were determined using two-way testing with a permutation-based FDR of 0.05 and a Log₂ *t*-test difference filter of 0.5.

upregulated proteins with the highest fold change, six were involved in the autophagic process, including SQSTM1 and LC3B.

We next assessed the effect of palmostatin B treatment on autophagy induction after a 4 h starvation in Earles Balanced Salt Solution (EBSS), with and without blockage of late-stage autophagy using 500 nM Bafilomycin A1 (BafA1). To measure autophagy, SQSTM1 and LC3-II levels were assessed via immunoblotting and immunofluorescence microscopy. EBSS treatment alone increased LC3-II and SQSTM1 levels as expected (Figure 2); however, the addition of palmostatin B led to a reduction in SQSTM1 and LC3-II levels in EBSS versus control conditions. The addition of BafA1 to block turnover increased the level of LC3-II. Together, these data indicate that inhibition of depalmitoylation causes a partial block in autophagy.

While the levels of LC3-II between different samples are a good measure of autophagic flux differences, we sought to determine if palmostatin B treatment changes the number of autophagosomes by measuring the number of LC3 and SQSTM1/p62 puncta using immunofluorescence microscopy. Palmostatin B treatment did not affect SQSTM1 puncta (Figure S1), but it did increase the number of LC3B puncta per cell (Figure S2). To assess the exact change in autophagy, a tandem LC3 reporter was employed (Figure 3). Palmostatin B did not alter autophagosome counts, though there was a significant increase in the number of autolysosomes (Figure 3). This increase in the later marker of autophagy suggests a late-stage blockage in autophagy, which is in line with our immunoblotting data.

3.2 | Palmitoylated SQSTM1 Is Degraded by the Lysosome

In contrast to LC3, until recently, SQSTM1 had not been shown to undergo any lipid modifications. However, it has been identified as potentially palmitoylated in several S-acyl proteome studies [8, 19]. Consequently, we sought to investigate if SQSTM1 undergoes S-acylation. HeLa cells were induced to undergo autophagy by serum deprivation in the presence or absence of BafA1 to prevent SQSTM1 degradation in the lysosome. Palmitoylation was detected using acyl-RAC. In the absence of autophagy or BafA1, low-level palmitoylation of SQSTM1 was detected (Figure 4). Serum deprivation led to a modest increase in SQSTM1 palmitoylation with a concomitant decrease in total SQSTM1 protein, suggesting palmitoylated SQSTM1 is directed to the lysosome where it is degraded. The addition of BafA1 significantly increased SQSTM1 palmitoylation, further confirming that palmitoylated SQSTM1 is directed to the lysosome but cannot be degraded when fusion between the lysosome and autophagosome is blocked with BafA1. No effect of palmitoylation was detected for the well-characterized Ras protein [10, 34], confirming the palmitoylation of SQSTM1 was specific to autophagy induction.

3.3 | SQSTM1 Palmitoylation at the C289,290 Di-Cysteine Motif Is Required for Delivery to the Lysosome

Palmitoylation of SQSTM1 is predicted (CSS-Palm 3.0 and 4.0) [35] to occur at two di-cysteine motifs: C26,27 and C289,290.

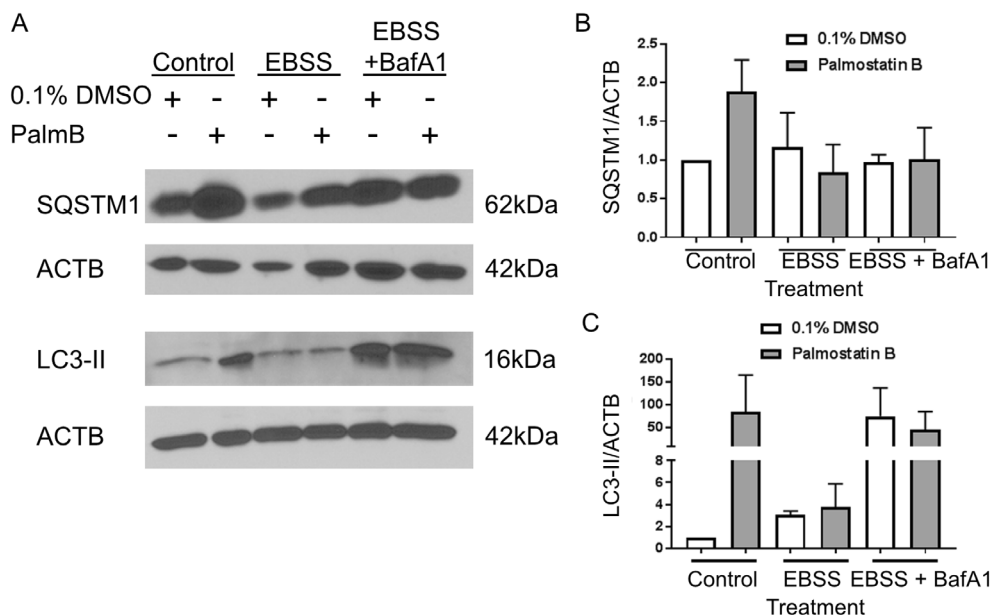


FIGURE 2 | Palmostatin B alters autophagy in HeLa cells, assessed through LC3B and SQSTM1 immunoblotting. HeLa cells were treated with 0.1% DMSO or 100 μ M palmostatin B (PalmB) for 18 h. Autophagy was induced by 4 h EBSS treatment or induced and inhibited by 4 h EBSS/2 h treatment with 500 nM BafA1. (A) Representative images of immunoblotting conducted for autophagy markers SQSTM1 and LC3-II with and without Palm B treatment and autophagy induction. (B) Quantification of immunoblots for SQSTM1 normalized to ACTB/ β -actin. Densitometry was conducted using ImageJ software (mean \pm SEM from three independent experiments; two-way ANOVA). (C) Quantification of immunoblots for LC3-II normalized to ACTB. Quantification was conducted using ImageJ software (mean \pm SEM from three independent experiments; two-way ANOVA).

Consequently, cysteine-to-serine mutations were made at both sites. Serine is more structurally similar to cysteine than other amino acids. Only the mutations at C289,290 significantly decreased palmitoylation of SQSTM1 (Figure 5A,B). This confirms the recent results from Huang et al. [22], published during the preparation of this manuscript. Palmitoylation was not completely abolished. Interestingly, palmitoylation did not increase in the presence of BafA1 in C289,290S, suggesting that this may be the site that directs SQSTM1 to the phagophore (the sequestering compartment that is the precursor to the autophagosome) and, ultimately, the lysosome (Figure 5A,B).

Upon autophagy induction, the C289,290S SQSTM1-HA mutant showed a slight reduction in colocalization with RFP-LC3 compared to WT SQSTM1-HA (Figure 5C,D). However, this effect was less pronounced than recently reported by Huang et al., possibly due to the use of *sqstm1*-KO cell lines in their study. They noted the importance of palmitoylated SQSTM1 for the association with and sequestration in the autophagic membranes [22]. In our WT HeLa cells, the endogenous SQSTM1 and the overexpressed C289,290S mutant can bind to LC3 via the LIR motif. Thus, palmitoylation of endogenous SQSTM1 may be enough to compensate for the defect in autophagosome formation caused by the lack of palmitoylation at the C289,290 site in overexpressed C289,290S cells. Since both endogenous SQSTM1 and the C289,290S mutant are present within the autophagosomes, a robust decrease in colocalization with RFP-LC3 was not observed compared to WT SQSTM1-HA (Figure 5C,D). Additionally, the colocalization between RFP-LC3 and the lysosomes slightly increased in C289,290S mutants compared to the WT SQSTM1-HA under

starvation-induced autophagy conditions (Figure 5F). An increase in the overlap between C289,290S SQSTM1-HA and the lysosomes was also observed compared to WT SQSTM1-HA under autophagy induction (Figure 5E). Thus, indicating that lack of palmitoylation may be hindering the lysosomal degradation, as previously reported [22]. Our data show that while endogenous SQSTM1 may compensate for the defects in autophagosome formation in C289,290S mutants, it cannot fully restore the lysosomal degradation. Together, these results suggest that the palmitoylation of SQSTM1 at the C289,290 motif is integral for the localization of SQSTM1 to both the autophagosomes and the lysosomes.

3.4 | Palmitoylation of SQSTM1 Is Decreased in Brains of HD Patients

Several studies have indicated a cargo-loading defect in cells derived from HD models and patients [23, 24, 36], leading to empty autophagosomes and a build-up of cytoplasmic debris, thereby contributing to the pathogenesis of HD. As a crucial receptor for autophagy that targets aggregated proteins, mutant HTT (huntingtin; mHTT), and damaged mitochondria [2, 27], we hypothesized that SQSTM1 palmitoylation is reduced in HD, which contributes to the empty autophagosome phenotype. As such, acyl-RAC was performed from donated HD patient brains to measure SQSTM1 palmitoylation. Palmitoylation of SQSTM1 was significantly reduced in the cortex from HD patients compared to unaffected controls (Figure 6A,B), despite a concomitant, but statistically insignificant, increase in total SQSTM1 levels.

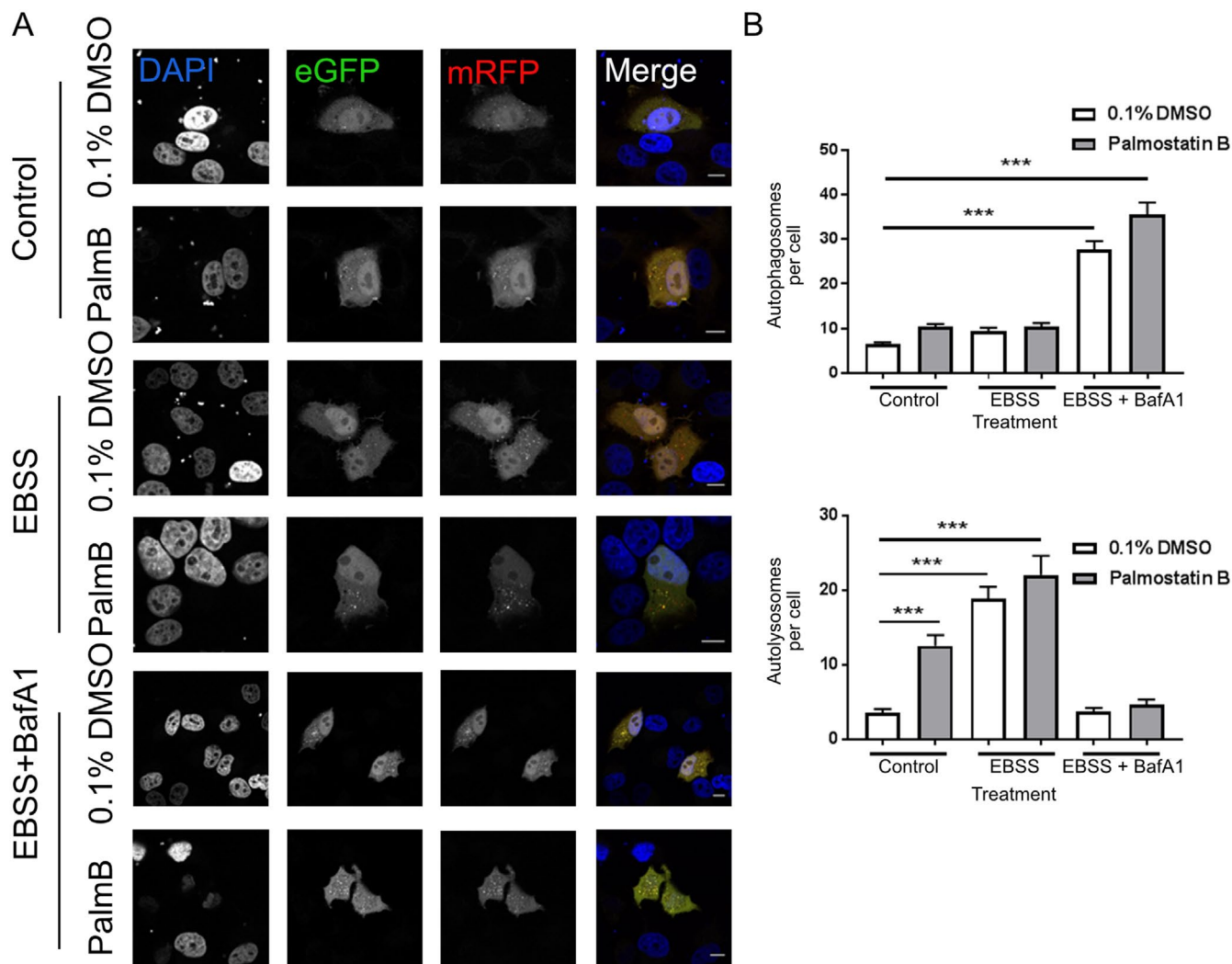


FIGURE 3 | Palmostatin B alters autophagy in HeLa cells, assessed through the tandem LC3 reporter. HeLa cells were treated with 0.1% DMSO or 100 μ M Palmostatin (PalmB) for 18 h. Autophagy was induced by 4 h EBSS treatment or induced and inhibited by 4 h EBSS and 2 h 500 nM BafA1. (A) Representative images of immunofluorescence conducted for eGFP-mRFP-LC3 after PalmB and autophagy treatment. (B) Quantification of the number of autophagosomes per cell (yellow puncta) and autolysosomes per cell (red puncta). Quantification was conducted on ImageJ software (mean \pm SEM from three independent experiments; two-way ANOVA; N (cells) Control: 123, Control + PalmB: 64, EBSS: 71, EBSS + Palm B: 44, Auto: 85, Auto + Palm B: 64) *** p < 0.001. Scale bars represent 10 μ m.

3.5 | Fasting-Induced Autophagy Rescues SQSTM1 Palmitoylation in the Brains of the YAC128 HD Mouse Model

Loss of SQSTM1 palmitoylation was also recapitulated in the brains from 8-month-old YAC128 HD mice by IP-ABE compared to wild-type (WT) control mice (Figure 6C,D). Here, palmitoylation was detected in the brains of 8-month-old mice by ABE following immunoprecipitation of SQSTM1. Mice were either kept on a regular diet or fasted overnight (24 h) to induce autophagy, as previously described [27]. Similar to HD patients, we detected a significant decrease in palmitoylation of SQSTM1 in the YAC128 HD mouse brains (black bars—Fed) compared to their WT littermates (White Bars—Fed).

Previously, we demonstrated that autophagy could be induced through fasting in the YAC128 mouse [27]. As such, SQSTM1 palmitoylation was assessed in fed and 24-h fasted WT and

YAC128 mice (Figure 6). Fasting rescued the decrease in SQSTM1 palmitoylation in YAC128 mouse brains to WT levels.

3.6 | Palmostatin B Treatment Improves Targeting of HTT to Lysosomes

We recently showed that increasing palmitoylation of mHTT, using palmotatin B, improved mHTT solubility and reduced toxicity [29]. Another study reported that improving overall palmitoylation in the brain improved phenotypes in HD mice [37]. These studies suggest that increasing palmitoylation may be a therapeutic target in HD. Our data have shown that palmitoylation of SQSTM1 is reduced in HD (Figure 6). We predict that increasing palmitoylation of SQSTM1 may improve the autophagy cargo-loading defect in HD and improve mHTT degradation. Therefore, we investigated the effect of

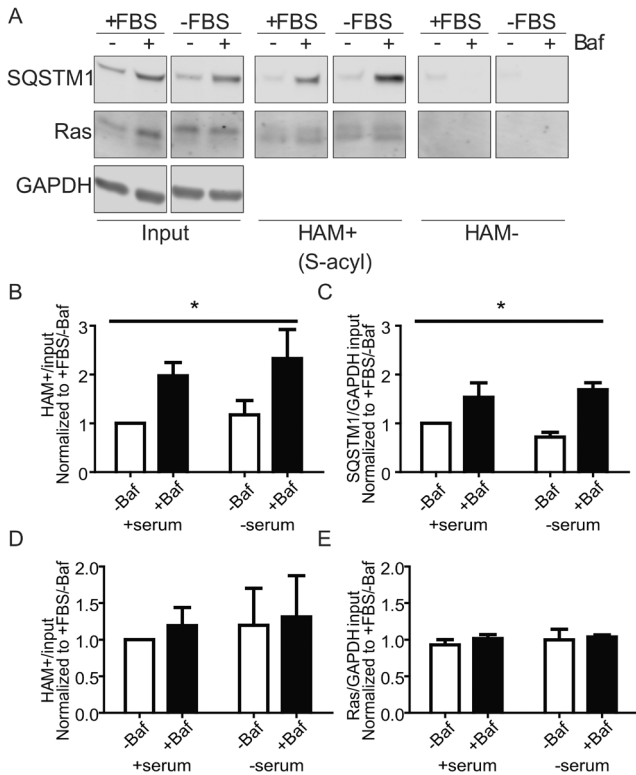


FIGURE 4 | SQSTM1 is palmitoylated and degraded by the lysosome. HeLa cells were induced to undergo autophagy through serum deprivation (–FBS) in the presence or absence of 400 nM BafA1. (A) Palmitoylation of SQSTM1 and Ras was detected by the acyl-RAC assay. Composite gel, all samples were run on the same gel. (B) During autophagy SQSTM1 palmitoylation increased while (C) total SQSTM1 levels decreased (degraded by the lysosome). BafA1 significantly increased both (B) SQSTM1 palmitoylation and (C) total protein. (D) S-acylated Ras and (E) protein levels were not significantly affected by either serum deprivation or BafA1 (two-way ANOVA, $n = 3$, SEM, $*p < 0.05$).

increasing palmitoylation on the localization of HTT and SQSTM1 to the lysosomes. In HeLa cells treated with palmostatin B, there was a robust increase in the colocalization between SQSTM1 and the lysosomes, as well as between HTT and lysosomes (Figure 7A,C,D). There was a significant increase in the overlap between SQSTM1 and HTT indicating an improvement in the potential interaction between the two proteins (Figure 7B). Together, these results suggest that increasing palmitoylation increases the localization of SQSTM1 to the autophagosomes and therefore, the targeting of HTT to the autophagosomes which in turn improves the localization of HTT to lysosomes, where it can be degraded.

4 | Discussion

The significant enrichment of palmitoylated proteins in autophagy, as identified by our bioinformatics approach [5, 8] and increase of autophagy proteins in response [5] to the depalmitoylation inhibitor palmostatin B, suggests that palmitoylation likely plays an important role in regulating autophagy. Palmitoylation likely regulates autophagy by acting as a mechanism for autophagy regulators to quickly localize to and from

membranes during the induction of autophagy. Recently, other regulators of autophagy have been shown to be palmitoylated, including AKT, MTOR, CALCOCO2, ULK1, and LAMTOR1 [21, 38, 39]. We predict that negative regulators of autophagy found at membrane interfaces, like MTOR, are palmitoylated when active and depalmitoylated when autophagy is activated. Conversely, we predict that autophagy regulators that need to quickly localize to membranes (i.e., LC3 lipidating enzymes, SQSTM1, etc.) are palmitoylated when autophagy is activated. Additionally, some proteins could also act as lipid sensors. For example, the LC3 lipidating enzymes have active cysteines that may be palmitoylated and inactive in the absence of autophagy. Fasting may promote their depalmitoylation and subsequent activation and lipidation of LC3.

Our data indicate two potential processes by which palmostatin B-mediated increases in palmitoylation may cause altered autophagy. Increased palmitoylation either causes an overall increase in autophagy or it causes a late-stage autophagy blockage. Although it is clear enhanced palmitoylation influences autophagy levels, we sought to examine the mechanism behind this. We found clear differences in autophagy proteins LC3 and SQSTM1 after upregulation of palmitoylation via palmostatin B treatment. Due to the important link between SQSTM1 and HTT, we chose to determine if SQSTM1 was in fact palmitoylated. Subsequently, we confirmed that it is modified via palmitoylation (Figure 4) and showed that it is regulated by autophagy induction. Blocking the fusion between autophagosomes and lysosomes led to an increase in SQSTM1 levels and palmitoylation, suggesting that lipidated SQSTM1 is directed to phagophores as is lipidated LC3. Although SQSTM1 has LC3-interacting motifs [23, 40], palmitoylation may provide the initial or additional signal that brings LC3 and SQSTM1 into proximity to interact. Palmitoylation may also provide an LC3-independent mechanism to direct SQSTM1 to the phagophore. Studying SQSTM1 palmitoylation is complicated by the fact that autophagosome-directed SQSTM1 is ultimately degraded by the lysosome. Therefore, it is difficult to detect SQSTM1 palmitoylation without blocking the fusion between the autophagosome and lysosome with compounds such as BafA1. In turn, inducing SQSTM1 palmitoylation presumably leads to degradation of SQSTM1, making it harder to detect.

Wildtype HTT is involved in regulating basal or bulk autophagy, while mHTT is associated with defects in autophagosomal and lysosomal fusion [2, 23, 36, 41]. In combination with the known cargo-binding defect [23, 24], this is likely why inducing autophagy in HD is not efficient and potentially toxic, akin to adding water to a clogged sink. As such, this is why we determined that the best method to remove mHTT was to promote fasting-induced autophagy, an HTT-independent pathway [27]. This may partly explain why mHTT is lowered in the brains of YAC128 mice when autophagy is induced through a week-long intermittent fasting paradigm. Similarly, herein, a short fasting time increased the palmitoylation of mHTT in the brains of YAC128 mice. Therefore, fasting-induced autophagy may also correct the cargo-loading defect seen in HD by increasing SQSTM1 palmitoylation and localization to the autophagosome and lysosome for degradation.

Similar to SQSTM1, we have previously shown that mHTT palmitoylation is lower in several models of HD, including

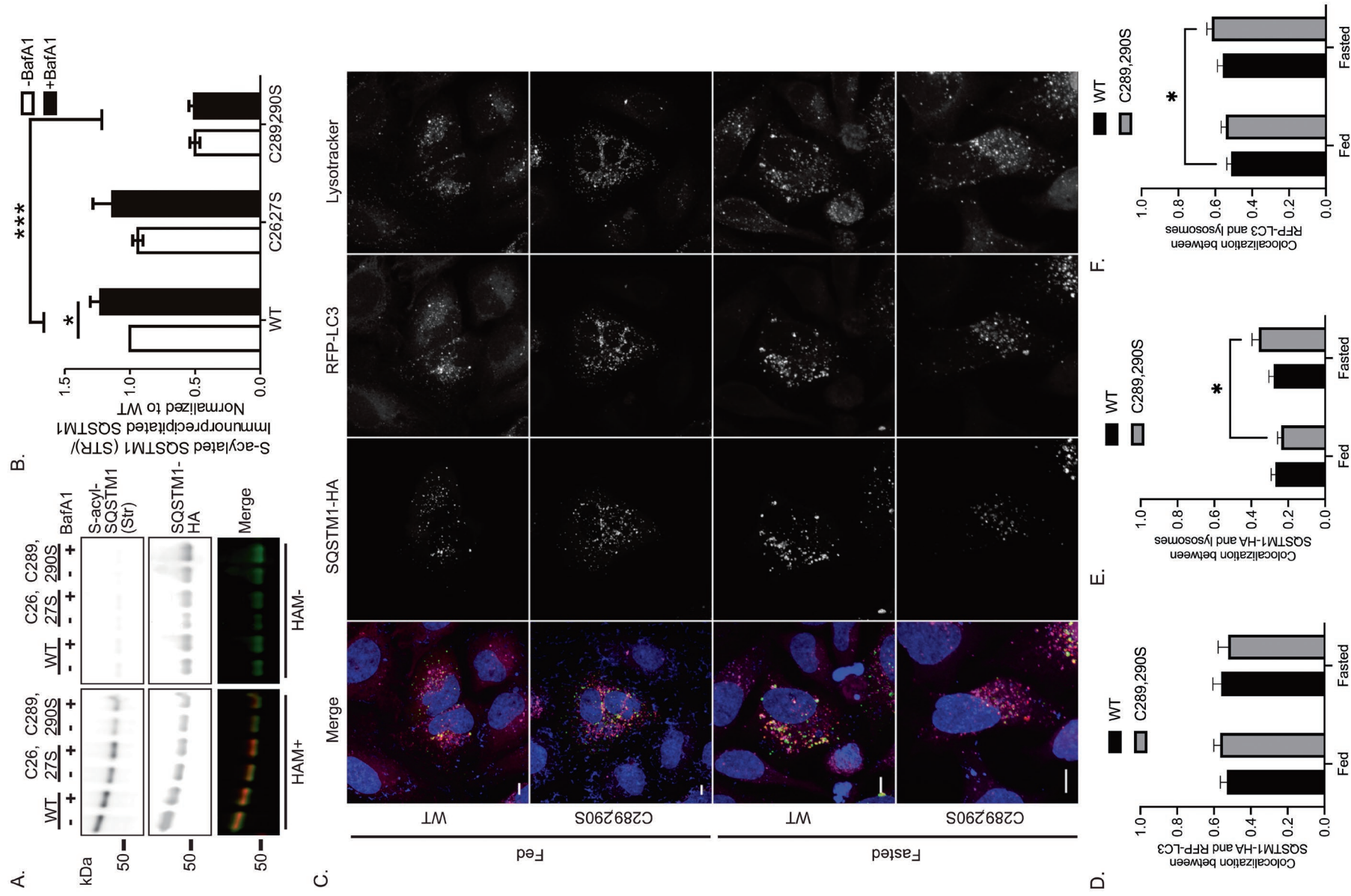


FIGURE 5 | Legend on next page.

FIGURE 5 | SQSTM1 is palmitoylated at the di-cysteine C289, 290 motif, which is required for localization to the lysosome. (A) IP-ABE was performed from transfected HeLa cells expressing the indicated forms of SQSTM1-HA in the presence or absence of BafA1 and palmitoylation was detected by streptavidin (STR). Composite gel, all samples were run on the same gel. (B) Only mutation of the C289, 290 di-cysteine motif significantly reduced S-acylation of SQSTM1-HA, regardless of the addition of BafA1 ($n = 4-7$, $* < 0.05$, $*** < 0.0001$, two-way ANOVA). (C) HeLa cells expressing RFP-LC3 (autophagosome marker) and the indicated SQSTM1-HA were stained with Lysotracker Far Red for 1-h prior to fixation. Cells were either grown in complete media (fed) as a control or subjected to growth in serum-deprived media (fasted) for 4h to induce autophagy and visualized by confocal microscopy ($n = 3$). Scale bar = 10 μm . Co-localization was measured as Pearson's colocalization coefficient (PCC) for (D) SQSTM1-HA and RFP-LC3, (E) SQSTM1-HA and lysosomes, and (F) RFP-LC3 and lysosomes. Statistical significance was determined by two-way ANOVA with Bonferroni's post hoc comparison; $*p < 0.05$. Data are represented as mean \pm SEM.

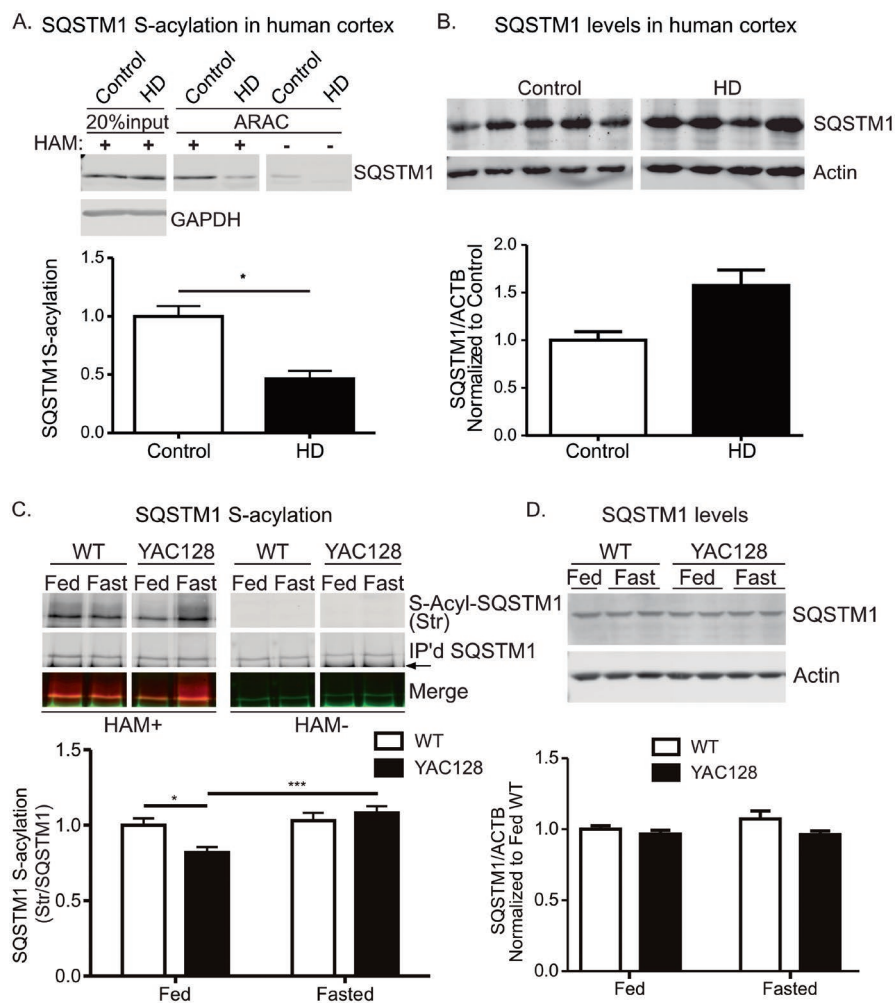


FIGURE 6 | SQSTM1 palmitoylation is significantly reduced in HD. (A, B) SQSTM1 palmitoylation is significantly reduced in the cortex from HD patient brains. (A) Palmitoylation of SQSTM1 was detected in patient brains by acyl-resin assisted capture (ARAC). Tissues used were from patients of similar age at death, CAG size, and post-mortem interval. Male and female samples were included in controls and HD samples. Two-tailed unpaired t -test, SEM ($n = 5,4$ for Ctrl, HD). Composite gel, all samples were run on the same gel. (B) Total SQSTM1 levels were examined in HD patients. (C, D) Significantly reduced SQSTM1 palmitoylation in the brains of HD mice is restored by fasting. Eight-month-old YAC128 mice were fasted for 24h, as previously described. (C) Palmitoylation of SQSTM1 was detected using IP-ABE (SQSTM1 is immunoprecipitated prior to ABE—top) and quantified (bottom). The arrow on the blot indicates the antibody heavy chain band. Composite gel, all samples were run on the same gel. (D) Total SQSTM1 levels were immunodetected (top) and quantified (bottom). Statistical significance was determined by two-way ANOVA with Bonferroni's post hoc comparison; $*p < 0.05$, $***p < 0.0001$. Data are represented as SEM.

patient-derived lymphoblastoid cells and stem cells [29, 42]. Blocking depalmitoylation with the broad inhibitor palmostatin B decreased insoluble mHTT and increased HTT palmitoylation with a concomitant increase in cell survival in primary neuronal cells derived from the YAC128 HD mouse model [29]. An independent study verified the protective effects of blocking depalmitoylation [37]. Although the latter study did not directly measure

palmitoylation, these studies [29, 37] combined suggest that promoting palmitoylation in HD is protective [43]. Our data suggest that the protective effect may also be due to increased SQSTM1 palmitoylation that directs mHTT to the autophagosome for degradation since inhibiting depalmitoylation with palmostatin B increased HTT localization to the lysosomes. However, it is unclear if palmostatin B is safe for long-term use in mice or humans.

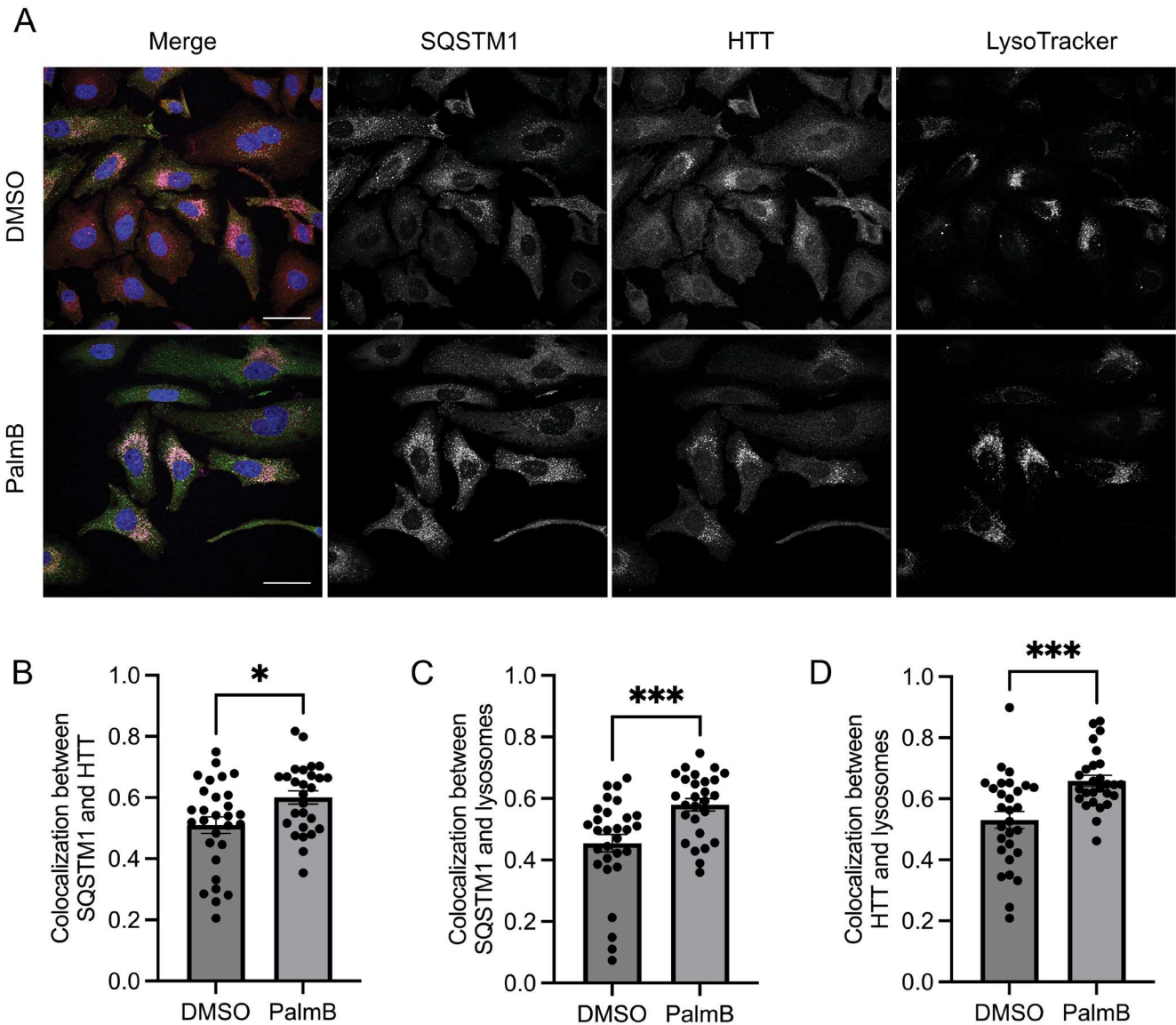


FIGURE 7 | Palmostatin B increases localization of HTT to the autophagosomes. HeLa cells were treated with 0.1% DMSO or 10 μ M Palmostatin B (PalmB) for 16–18 h. (A) Representative images of immunofluorescence conducted on the treated cells for endogenous SQSTM1 and endogenous HTT. Lysosomes were stained with 50 nM LysoTracker Far Red (ThermoFisher Scientific, L12492); 1 h incubation at 37°C prior to fixation. Scale bar = 50 μ m. Co-localization was measured as Pearson's colocalization coefficient (PCC) for (B) SQSTM1 and HTT, (C) SQSTM1 and lysosomes, and (D) HTT and lysosomes. Statistical significance was determined by the two-tailed unpaired *t*-test; * $p < 0.05$, *** $p < 0.001$. Data are represented as mean \pm SEM ($n = 3$).

Future studies into the safety of palmostatin B are needed. More specific inhibitors, like ML348, may be required for longer treatments but still require further investigation. As novel inhibitors for palmitoylation and depalmitoylation continue to emerge, we will need to assess this further and confirm that the effects in the nervous system match those in peripheral tissues. Both HTT and SQSTM1 are ubiquitously expressed throughout the body, as are many of the proteins mutated in neurodegenerative diseases [5, 44]. To date, we have detected decreased mutant HTT palmitoylation in peripheral (patient lymphoblasts) and nervous tissues. Therefore, it is expected that rescuing mutant HTT and SQSTM1 palmitoylation systemically would be protective.

Ultimately, the data presented herein suggest that approaches promoting SQSTM1 palmitoylation may be beneficial in HD.

Of note, many mutations in SQSTM1 are associated with ALS, frontotemporal dementia, and Charcot–Marie Tooth disease [45], and SQSTM1 deposits are also hallmark features of ALS, Charcot–Marie Tooth disease, and multisystem proteinopathy [46, 47]. Therefore, palmitoylation of SQSTM1 may be a potential marker for disease, and modulating SQSTM1 palmitoylation may be an attractive therapeutic approach in multiple disorders. It will be important to investigate if SQSTM1 palmitoylation is altered in these diseases and how it is regulated.

Author Contributions

F.A., M.C.D., D.D.O.M., S.S.S., and M.O.C. contributed to the preparation of the manuscript and experimental design. J.C. helped with

identifying tissues and maintaining the brain bank. N.S.C. helped with animal studies. Y.T.N.N. helped complete biochemical studies represented in Figures 3–6. A.K., A.D., Y.A., and F.A. completed microscopy imaging in Figures 5 and 7. M.C.D. contributed to Figures 1–3, S1, and S2. J.S.C. contributed to proteomic studies. M.R.H. provided patient and animal tissues and support to trainees.

Acknowledgments

The authors would like to thank members of the Hayden lab for helpful discussions and input. In particular, Mahsa Amir, Mark Wang, and Yun Ko for organizing and maintaining mouse colonies and Dr. Amber Southwell for helpful comments for mouse studies. Thank you to Dr. Daniel Klionsky for your valuable feedback on the manuscript. The Summary Figure was provided by Cailyn Perry. Finally, we would like to thank all the patients and their families who donated tissues to help move HD research forward. This work could not have been done without them. M.O.C. and M.C.D. were supported by a grant from The Royal Society (RG150409). J.S.C. was supported by the Wellcome Trust (079643/Z/06/Z). D.D.O.M., F.A., and A.K. were supported by a Natural Sciences and Engineering Research Council (NSERC) Discovery Grant (RGPIN-2019-04617). M.R.H. was supported by funding from the Canadian Institutes of Health Research (CIHR, FDN: 154278). A.D. was supported by an NSERC-USRA and a summer fellowship from the Huntington Society of Canada. Y.A. is supported by a Canada Graduate Scholarship-Master's (CGS-M) from CIHR.

Conflicts of Interest

The authors declare no conflicts of interest.

Data Availability Statement

The data that support the findings of this study are available in the Materials and Methods, Results, and [Supporting Information](#) of this article.

References

1. T. R. Suk and M. W. C. Rousseaux, "The Role of TDP-43 Mislocalization in Amyotrophic Lateral Sclerosis," *Molecular Neurodegeneration* 15, no. 1 (2020): 1–16, <https://doi.org/10.1186/s13024-020-00397-1>.
2. D. D. O. Martin, S. Ladha, D. E. Ehrnhoefer, and M. R. Hayden, "Autophagy in Huntington Disease and Huntingtin in Autophagy," *Trends in Neurosciences* 38 (2015): 26–35.
3. M. Zatyka, S. Sarkar, and T. Barrett, "Autophagy in Rare (NonLysosomal) Neurodegenerative Diseases," *Journal of Molecular Biology* 432 (2020): 2735–2753.
4. F. M. Menzies, A. Fleming, A. Caricasole, et al., "Autophagy and Neurodegeneration: Pathogenic Mechanisms and Therapeutic Opportunities," *Neuron* 93, no. 5 (2017): 1015–1034, <https://doi.org/10.1016/j.neuron.2017.01.022>.
5. F. Ramzan, F. Abrar, G. G. Mishra, L. M. Q. Liao, and D. D. O. Martin, "Lost in Traffic: Consequences of Altered Palmitoylation in Neurodegeneration," *Frontiers in Physiology* 14 (2023): 1166125.
6. A. K. H. Stavoe and E. L. F. Holzbaur, "Autophagy in Neurons," *Annual Review of Cell and Developmental Biology* 35 (2019): 477–500.
7. D. J. Klionsky, G. Petroni, R. K. Amaravadi, et al., "Autophagy in Major Human Diseases," *EMBO Journal* 40, no. 19 (2021): 1–63, <https://doi.org/10.15252/embj.2021108863>.
8. S. S. F. Sanders, D. D. O. Martin, S. L. Butland, et al., "Curation of the Mammalian Palmitoylome Indicates a Pivotal Role for Palmitoylation in Diseases and Disorders of the Nervous System and Cancers," *PLoS Computational Biology* 11, no. 8 (2015): e1004405, <https://doi.org/10.1371/journal.pcbi.1004405>.

9. D. A. Mitchell, A. Vasudevan, M. E. Linder, and R. J. Deschenes, "Thematic Review Series: Lipid Posttranslational Modifications. Protein Palmitoylation by a Family of DHHC Protein S-Acyltransferases: Fig. 1," *Journal of Lipid Research* 47 (2006): 1118–1127.
10. M.-E. Zaballa and F. G. van der Goot, "The Molecular Era of Protein S-Acylation: Spotlight on Structure, Mechanisms, and Dynamics," *Critical Reviews in Biochemistry and Molecular Biology* 53 (2018): 1–31.
11. A. Main and W. Fuller, "Protein S-Palmitoylation: Advances and Challenges in Studying a Therapeutically Important Lipid Modification," *FEBS Journal* 289 (2022): 861–882.
12. D. T. Lin and E. Conibear, "ABHD17 Proteins Are Novel Protein Depalmitoylases That Regulate N-Ras Palmitate Turnover and Subcellular Localization," *eLife* 4 (2015): e11306, <https://doi.org/10.7554/eLife.11306>.
13. L. A. Camp and S. L. Hofmann, "Purification and Properties of a Palmitoyl-Protein Thioesterase That Cleaves Palmitate From H-Ras," *Journal of Biological Chemistry* 268 (1993): 22566–22574.
14. J. A. Duncan and A. G. Gilman, "A Cytoplasmic Acyl-Protein Thioesterase That Removes Palmitate From G Protein α Subunits and P21RAS," *Journal of Biological Chemistry* 273 (1998): 15830–15837.
15. A. F. Roth, J. Wan, A. O. Bailey, et al., "Global Analysis of Protein Palmitoylation in Yeast," *Cell* 125, no. 5 (2006): 1003–1013, <https://doi.org/10.1016/j.cell.2006.03.042>.
16. Y. Fukata and M. Fukata, "Protein Palmitoylation in Neuronal Development and Synaptic Plasticity," *Nature Reviews Neuroscience* 11 (2010): 161–175.
17. H. J. Kim, A. A. Soyombo, S. Tjon-Kon-Sang, I. So, and S. Muallem, "The $ca(2+)$ Channel TRPML3 Regulates Membrane Trafficking and Autophagy," *Traffic* 10 (2009): 1157–1167.
18. M. Park, A. Sabetski, Y. Kwan Chan, S. Turdi, and G. Sweeney, "Palmitate Induces ER Stress and Autophagy in H9c2 Cells: Implications for Apoptosis and Adiponectin Resistance," *Journal of Cellular Physiology* 230 (2015): 630–639.
19. M. Blanc, F. David, L. Abrami, et al., "SwissPalm: Protein Palmitoylation Database," *F1000Research* 4 (2015): 1–23, <https://doi.org/10.12688/f1000research.6464.1>.
20. D. Türei, L. Földvári-Nagy, D. Fazekas, et al., "Autophagy Regulatory Network — A Systems-Level Bioinformatics Resource for Studying the Mechanism and Regulation of Autophagy," *Autophagy* 11 (2015): 155–165.
21. S. S. Sanders, F. I. De Simone, and G. M. Thomas, "mTORC1 Signaling Is Palmitoylation-Dependent in Hippocampal Neurons and Non-Neuronal Cells and Involves Dynamic Palmitoylation of LAMTOR1 and mTOR," *Frontiers in Cellular Neuroscience* 13 (2019), <https://www.frontiersin.org/journals/cellular-neuroscience/articles/10.3389/fncel.2019.00115/full>.
22. X. Huang, J. Yao, L. Liu, et al., "S-Acylation of p62 Promotes p62 Droplet Recruitment Into Autophagosomes in Mammalian Autophagy," *Molecular Cell* 83 (2023): 3485–3501.e11.
23. M. Martinez-Vicente, Z. Talloczy, E. Wong, et al., "Cargo Recognition Failure Is Responsible for Inefficient Autophagy in Huntington's Disease," *Nature Neuroscience* 13 (2010): 567–576.
24. C. Walter, L. E. Clemens, A. J. Müller, et al., "Activation of AMPK-Induced Autophagy Ameliorates Huntington Disease Pathology In Vitro," *Neuropharmacology* 108 (2016): 24–38.
25. W. Fan, Z. Tang, D. Chen, et al., "Keap1 Facilitates p62-Mediated Ubiquitin Aggregate Clearance via Autophagy," *Autophagy* 6 (2010): 614–621.
26. S. Kimura, T. Noda, and T. Yoshimori, "Dissection of the Autophagosome Maturation Process by a Novel Reporter Protein, Tandem Fluorescent-Tagged LC3," *Autophagy* 3 (2007): 452–460.

27. D. E. Ehrnhoefer, D. D. O. Martin, M. E. Schmidt, et al., "Preventing Mutant Huntingtin Proteolysis and Intermittent Fasting Promote Autophagy in Models of Huntington Disease," *Acta Neuropathologica Communications* 6, no. 16 (2018), <https://doi.org/10.1186/s40478-018-0518-0>.
28. M. O. Collins, K. T. Woodley, and J. S. Choudhary, "Global, Site-Specific Analysis of Neuronal Protein S-Acylation," *Scientific Reports* 7 (2017): 4683.
29. F. L. Lemarié, N. S. Caron, S. S. Sanders, et al., "Rescue of Aberrant Huntingtin Palmitoylation Ameliorates Mutant Huntingtin-Induced Toxicity," *Neurobiology of Disease* 158 (2021): 105479.
30. S. S. Sanders, M. P. Parsons, K. K. N. Mui, et al., "Sudden Death due to Paralysis and Synaptic and Behavioral Deficits When Hip14/Zdhhc17 Is Deleted in Adult Mice," *BMC Biology* 14 (2016): 108.
31. F. L. Lemarié, S. S. Sanders, Y. Nguyen, D. D. O. Martin, and M. R. Hayden, "Full-Length Huntingtin Is Palmitoylated at Multiple Sites and Post-Translationally Myristoylated Following Caspase-Cleavage," *Frontiers in Physiology* 14 (2023): 1086112.
32. J. Schindelin, I. Arganda-Carreras, E. Frise, et al., "Fiji: An Open-Source Platform for Biological-Image Analysis," *Nature Methods* 9 (2012): 676–682.
33. D. D. O. Martin, S. M. Holland, S. S. Sanders, et al., "Identification of Novel Inhibitors of DLK Palmitoylation and Signaling by High Content Screening," *Scientific Reports* 9, no. 1 (2019): 3632, <https://doi.org/10.1038/s41598-019-39968-8>.
34. M. E. Linder and R. J. Deschenes, "Palmitoylation: Policing Protein Stability and Traffic," *Nature Reviews Molecular Cell Biology* 8 (2007): 74–84.
35. J. Ren, L. Wen, X. Gao, C. Jin, Y. Xue, and X. Yao, "CSS-Palm 2.0: An Updated Software for Palmitoylation Sites Prediction," *Protein Engineering, Design and Selection* 21 (2008): 639–644, <https://doi.org/10.1093/protein/gzn039>.
36. Y.-N. Rui, Z. Xu, B. Patel, A. M. Cuervo, and S. Zhang, "HTT/Huntingtin in Selective Autophagy and Huntington Disease: A Foe or a Friend Within?," *Autophagy* 11 (2015): 858–860.
37. A. Virlogeux, C. Scaramuzzino, S. Lenoir, et al., "Increasing Brain Palmitoylation Rescues Behavior and Neuropathology in Huntington Disease Mice," *Science Advances* 7, no. 14 (2021): eabb0799, <https://doi.org/10.1126/sciadv.abb0799>.
38. M. Blaustein, E. Piegari, C. Martínez Calejman, et al., "Akt Is S-Palmitoylated: A New Layer of Regulation for Akt," *Frontiers in Cell and Developmental Biology* 9 (2021): 1–16, <https://doi.org/10.3389/fcell.2021.626404>.
39. T. M. Nthiga, B. K. Shrestha, J.-A. Bruun, K. B. Larsen, T. Lamark, and T. Johansen, "Regulation of Golgi Turnover by CALCOCO1-Mediated Selective Autophagy," *Journal of Cell Biology* 220, no. 6 (2021): e202006128, <https://doi.org/10.1083/jcb.202006128>.
40. T. Johansen and T. Lamark, "Selective Autophagy Goes Exclusive," *Nature Cell Biology* 16 (2014): 395–397.
41. J. Ochaba, T. Lukacsovich, G. Csikos, et al., "Potential Function for the Huntingtin Protein as a Scaffold for Selective Autophagy," *Proceedings of the National Academy of Sciences* 111 (2014): 16889–16894.
42. A. Yanai, K. Huang, R. Kang, et al., "Palmitoylation of Huntingtin by HIP14 Is Essential for Its Trafficking and Function," *Nature Neuroscience* 9 (2006): 824–831.
43. D. D. O. Martin and S. S. Sanders, "Let's Get Fat: Emergence of S-Acylation as a Therapeutic Target in Huntington Disease," *Biochemical Society Transactions* 52 (2024): 1385–1392.
44. J. Wlodarczyk, R. Bhattacharyya, K. Dore, et al., "Altered Protein Palmitoylation as Disease Mechanism in Neurodegenerative Disorders," *Journal of Neuroscience* (2024), <https://www.jneurosci.org/content/44/40/e1225242024>.
45. J. Van Der Zee, T. Van Langenhove, G. G. Kovacs, et al., "Rare Mutations in SQSTM1 Modify Susceptibility to Frontotemporal Lobar Degeneration," *Acta Neuropathologica* 128, no. 3 (2014): 397–410, <https://doi.org/10.1007/s00401-014-1298-7>.
46. L. Wang, K. B. Ebrahimi, M. Chyn, M. Cano, and T. James, "Biology of p62/Sequestosome-1 in Age-Related Macular Degeneration (AMD)," in *Retinal Degenerative Diseases: Mechanisms and Experimental Therapy* (2016), 17–22, <https://doi.org/10.1007/978-3-319-17121-0>.
47. E. T. Cirulli, B. N. Lasseigne, S. Petrovski, et al., "Exome Sequencing in Amyotrophic Lateral Sclerosis Identifies Risk Genes and Pathways," *Science (New York, N.Y.)* 347, no. 6229 (2015): 1436–1441, <https://doi.org/10.1126/science.aaa3650>.

Supporting Information

Additional supporting information can be found online in the Supporting Information section.